# Application of the Variational Theorem for Creep of Shallow Spherical Shells

JOHN J. J. SHI,* CONOR D. JOHNSON,* AND NELSON R. BAULD JR.†
*Clemson University, Clemson, S.C.*

**The variational theorem for creep is used to study the creep deflections and collapse times for simply supported thin shallow spherical shells under uniform external pressure. The initial and subsequent forms of the stress resultants and displacements are obtained with the aid of the elastic theory of thin shallow spherical shells. The variational theorem for creep leads to a set of simultaneous ordinary differential equations with prescribed initial conditions. Numerical solutions are generated by means of the Runge-Kutta method. Theoretical predictions for creep deflections and collapse times are compared with experimental data for five test shells at each of three different pressure levels for Type 6/6 Nylon. It was found that the theory predicts creep deflections that are consistently smaller than the experimental values, whereas the theoretical collapse times are consistently larger than the experimental collapse times. The discrepancy between the theoretical predictions for creep deflections and collapses times and the experimental data is believed to be due largely to the deviations which occur between the theoretical and actual stress and displacement mode shapes with the passage of time. Closer agreement should be expected when more time flexibility is built into these mode forms.**

## Nomenclature

$A_i$ = coefficients appearing in approximating polynomials ($i = 1, 2, \ldots, 12$)
$a$ = radius of the projection of the shell onto its baseplane
$B$ = parameter defined by $B = (1 - \nu)qR^2\alpha_0/(2Eh)$
$C_0,p,\eta_0,\lambda,m$ = creep parameters
$D$ = flexural rigidity defined by $D = Eh^3/[12(1 - \nu^2)]$
$E,\nu$ = Young's modulus and Poisson's ratio, respectively
$h,R,H$ = shell thickness, radius of curvature, and rise, respectively
$I$ = creep functional
$I_i$ = coefficients arising through integration of creep functional ($i = 1, 2, \ldots, 31$)
$J_2$ = second invariant of the deviatoric stress tensor
$M_\rho,M_\theta$ = radial and circumferential moment resultants, respectively
$N_\rho,N_\theta$ = radial and circumferential force resultants, respectively
$q$ = external pressure
$q_{cr}$ = instantaneous critical pressure
$r$ = dimensionless radial coordinate defined by $r = \rho/a$
$S_{ij}$ = components of the deviatoric stress tensor
$S_d,S_s$ = portions of the surface over which the displacement and stress vectors are prescribed, respectively
$T_i$ = components of the surface traction
$T_i^*$ = prescribed components of the surface traction
$t$ = time, hours
$U,W$ = meridional and transverse components of displacement of a generic point in the shell
$u,w$ = meridional and transverse components of displacement of points lying on the middle surface of the shell
$U_i$ = components of the generic displacement vector
$U_i^*$ = prescribed components of the displacement vector
$\alpha$ = dimensionless variable defined by $\alpha = \rho/\rho_0$
$\alpha_0$ = parameter defined by $\alpha_0 = a/\rho_0$
$\delta_{ij}$ = Kronecker delta
$\epsilon_\rho,\epsilon_\theta$ = meridional and circumferential components of strain at a generic point in the shell, respectively
$\epsilon_{ij}$ = components of the total strain tensor
$\epsilon_{ije},\epsilon_{ijc}$ = components of the elastic and creep portions of the total strain tensor, respectively
$\rho,\theta,z$ = cylindrical coordinates
$\rho_0$ = parameter defined by $\rho_0^4 = DR^2/(Eh)$
$\sigma_\rho,\sigma_\theta$ = meridional and circumferential components of stress, respectively
$\sigma_{ij}$ = components of the stress tensor
$\Phi$ = Airy stress function

Received February 13, 1969; revision received July 17, 1969. This work was supported by the National Science Foundation under Grant GK-1832.

* Graduate Student, Department of Engineering Mechanics.
† Professor, Department of Engineering Mechanics.

## I. Introduction

A THIN shallow spherical shell under uniform pressure less than the instantaneous critical pressure is an example of a structural element which, prior to creep deformations, is stable in the classical sense but which ultimately deforms into a configuration that is unstable under the same external pressure, provided this pressure induces stresses that exceed the creep limit of the material. In some cases it is quite possible that the stresses accompanying the instantaneous critical pressure do not exceed the creep limit of the material, and, hence, all configurations for $q < q_{cr}$ represent stable and time-independent equilibrium configurations. In other cases the internal stresses accompanying the instantaneous critical pressure will exceed the creep limit of the material to the extent that for a small range of external pressures less than $q_{cr}$, creep deformations will be possible. Thus, with the passage of time a configuration that is initially stable will pass subsequently into an unstable configuration.

It is this last phenomenon to which the present investigation addresses itself. Accordingly, the purpose of this investigation is to study, via the variational theorem for creep,[1] transient and steady-state creep deformations and collapse times for simply supported thin shallow spherical shells under uniform external pressure. A further purpose is to present a comparison between theoretical predictions for creep deformations and collapse times with data obtained in the experimental phase of this investigation.

The procedure used in the application of the variational theorem for creep was to assume suitable approximate functions to represent the moment and force resultants and dis-

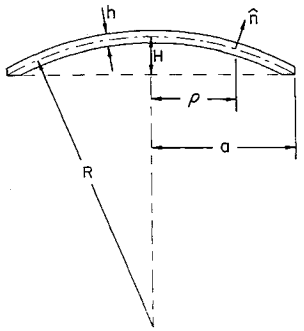


**Fig. 1 Sketch of shallow spherical shell showing pertinent geometric parameters and coordinates.**

placement components in the shell at an arbitrary time. The approximating functions were defined explicitly in the spatial coordinates using the elastic theory of thin shallow spherical shells[2,3] as a guide, whereas flexibility in the time coordinate is incorporated by means of dimensionless time parameters that are determined by the initial value problem that results from the application of the creep theorem. Initial values for the dimensionless time parameters are arrived at through the elastic theory of thin shallow spherical shells.

## II. Application of the Variational Theorem for Creep

### Geometrical Considerations

The pertinent geometrical parameters relevant to this study, as well as the coordinate system employed, are depicted in Fig. 1. It is assumed that the shell is subjected to a uniform external pressure that remains constant in magnitude and direction and is simply supported at the edge $\rho = a$. The coordinate system used is the customary one used in the study of the elastic theory of shallow shells with $\rho$, $\theta$ representing polar coordinates in the base-plane of the shell. Distance along the outwardly directed normal, measured from the middle surface of the shell, is denoted by positive $z$. Other important geometrical parameters are the shell rise $H$, thickness $h$, radius of curvature $R$, and base-plane edge radius $a$. The pressure is denoted by $q$.

### Variational Theorem for Creep

The variational theorem for creep asserts that, from among all admissible stress or strain rates for a known state of stress or strain, those which actually occur provide a stationary value to the creep functional.

The creep functional considered in the enunciation of the variational theorem is expressed in Cartesian tensor notation in the form

$$I = \int_v \{\dot{\epsilon}_{ij}\dot{\sigma}_{ij} + \tfrac{1}{2}\dot{U}_{k,i}\dot{U}_{k,j}\sigma_{ij} - \tfrac{1}{2}(\dot{\epsilon}_{ije} + 2\dot{\epsilon}_{ijc})\dot{\sigma}_{ij}\}dv - \int_{S_\sigma}\dot{T}_i{}^*\dot{U}_i ds - \int_{S_d}(\dot{U}_i - \dot{U}_i{}^*)\dot{T}_i ds \quad (1)$$

where dots over quantities signify differentiation with respect to time. Other symbols are defined in the Nomenclature accompanying this paper. According to this theorem, the first term in the volume integral is to be written in terms of displacements. The elastic part of the third term is to be written in terms of stress rates, and the creep part in terms of stresses. Finally, the creep functional is to be varied with respect to the time rates of change of the stresses and displacements and not the stresses and displacements themselves.

### Creep Model

The model used to represent the thin shallow spherical shell undergoing elastic and inelastic deformations assumes that the deformation (elastic and creep) occur in a rotationally symmetric manner, time-independent inelastic deformations are negligible, and a biaxial state of stress exists in the shell.

Strain-displacement relations used are those associated with the customary linearly elastic theory except that quadratic terms in the derivatives of the normal displacement $w$ are retained, thus

$$\epsilon_\rho = u_\rho + w/R + \tfrac{1}{2}w_\rho{}^2 - zw_{\rho\rho}, \qquad \epsilon_\theta = u/\rho + w/R - zw_\rho \quad (2)$$

Subscripts on displacements indicate differentiation; however, subscripts on other quantities such as stresses and strains indicate the coordinate directions with which these quantities are to be associated.

The displacements and stresses are assumed to vary over the thickness according to the relations

$$U = u - zw_\rho, \; W = w \quad (3)$$

and

$$\sigma_i(\rho,t) = [N_i(\rho,t)/h] + (12z/h^3)M_i(\rho,t), \qquad (i = \rho,\theta) \quad (4)$$

The quantities $N_i$ and $M_i$ are force and moment resultants defined in thin shell theory.[4]

The constitutive relations used in this study consist of Hooke's law for the elastic part of the total strain, and the following creep relation that determines the creep rates

$$\dot{\epsilon}_{ijc} = C_0 p t^{p-1} J_2{}^{\eta_0} S_{ij} \quad (5)$$

where $S_{ij}$ and $J_2$ represent the components of the deviatoric stress tensor and the second invariant of this tensor, respectively. The material properties $(C_0,p,\eta_0)$ are determined by requiring that the multiaxial creep relation Eq. (5) reduce to the uniaxial creep relation

$$\dot{\epsilon} = \lambda \sigma^m p t^{p-1} \quad (6)$$

The material properties $(\lambda,m,p)$ can be determined from a family of constant stress creep curves at constant temperature. The various material properties are interrelated by the formulas

$$\eta_0 = (m-1)/2, \; C_0 = (\lambda/2)3^{[(m+1)/2]} \quad (7)$$

### Construction of the Creep Functional

The only nonzero components of stress and displacement are the membrane stresses $\sigma_\rho$ and $\sigma_\theta$, and the meridional and transverse displacements $u$ and $w$. The various terms in the integrand of the volume integral of the creep functional are found to be (see Appendix A for the transformation of the second term from cartesian coordinates to the present system)

$$\dot{\epsilon}_{ij}\dot{\sigma}_{ij} = \left(\dot{u}_\rho + \frac{\dot{w}}{R} + w\dot{w}_\rho - z\dot{w}_{\rho\rho}\right)\dot{\sigma}_\rho + \left(\frac{\dot{u}}{\rho} + \frac{\dot{w}}{R} - \frac{z}{\rho}\dot{w}_\rho\right)\dot{\sigma}_\theta \quad (8)$$

$$\tfrac{1}{2}\dot{\epsilon}_{ije}\dot{\sigma}_{ij} = (1/2E)(\dot{\sigma}_\rho{}^2 - 2\nu\dot{\sigma}_\rho\dot{\sigma}_\theta + \dot{\sigma}_\theta{}^2) \quad (9)$$

$$\dot{\epsilon}_{ijc}\dot{\sigma}_{ij} = \frac{C_0 p t^{p-1}}{3\eta_0 + 1}(\sigma_\rho{}^2 - \sigma_\rho\sigma_\theta + \sigma_\theta{}^2)^{\eta_0} \times [(2\sigma_\rho - \sigma_\theta)\dot{\sigma}_\rho + (2\sigma_\theta - \sigma_\rho)\dot{\sigma}_\theta] \quad (10)$$

and

$$\dot{U}_{k,i}\dot{U}_{k,j}\sigma_{ij} = \left[\left(\dot{u}_\rho + \frac{\dot{w}}{R} - z\dot{w}_{\rho\rho}\right)^2 + \left(\dot{w}_\rho - \frac{\dot{u}}{R} + z\dot{w}_\rho\right)^2\right]\sigma_\rho + \frac{\dot{u}}{\rho} + \left(\frac{\dot{w}}{R} - \frac{z}{\rho}\dot{w}_\rho\right)^2\sigma_\theta \quad (11)$$

For thin shallow shells ($z/R \ll 1$ and $H/a \ll 1$) the volume element can be approximated by $dv = \rho d\rho d\theta dz$.

Making use of Eqs. (3) and the definition of the stress resultants of thin shell theory the surface integrals entering into the creep functional can be written in the form

$$\int_{S_\sigma} \dot{T}^* \dot{U}_i ds = \int_{S_\sigma} (\dot{T}_\rho^* \dot{U} + \dot{T}_\theta^* \dot{V} + \dot{T}_z^* W) ds \qquad (12)$$

and

$$\int_{S_d} (\dot{U}_i - \dot{U}_i^*) \dot{T}_i ds = \int_A \{(\dot{u} - \dot{u}^*) \dot{N}_\rho - (\dot{w}_\rho - \dot{w}_\rho^*) \dot{M}_\rho + (\dot{w} - \dot{w}^*) \dot{Q}_\rho\} dA \qquad (13)$$

Here $A$ signifies the region occupied by the base-plane of the shell. The pressure is assumed to remain constant in magnitude and direction, thus the integral (12) vanishes identically. The integral (13) supplies the conditions that are to be satisfied at the edge of the shell. Accordingly, for the simply supported shell the boundary conditions to be satisfied are $\dot{u}(a,t) = \dot{w}(a,t) = \dot{M}_\rho(a,t) = 0$. Introducing the dimensionless radial coordinate $r = \rho/a$ and integrating with respect to $\theta$, yields for the creep functional

$$I = 2\pi a^2 \int_{-h/2}^{h/2} \int_0^1 \left\{ \left( \frac{\dot{u}_r}{a} + \frac{\dot{w}}{R} + \frac{w_r \dot{w}_r}{a^2} - \frac{z}{a^2} \dot{w}_{rr} \right) \dot{\sigma}_\rho + \left( \frac{\dot{u}}{ar} + \frac{\dot{w}}{R} - \frac{z}{ra^2} \dot{w}_r \right) \dot{\sigma}_\theta + \frac{1}{2} \left[ \left( \frac{\dot{u}_r}{a} + \frac{\dot{w}}{R} - \frac{z}{a^2} \dot{w}_{rr} \right)^2 \sigma_\rho + \left( \frac{\dot{w}_r}{a} - \frac{\dot{u}}{R} + \frac{z}{aR} \dot{w}_r' \right)^2 \sigma_\rho + \left( \frac{\dot{w}}{R} + \frac{\dot{u}}{ar} - \frac{z}{ra^2} \dot{w}_r \right)^2 \sigma_\theta \right] - \frac{1}{2} (\dot{\sigma}_\rho^2 - 2\nu \dot{\sigma}_\rho \dot{\sigma}_\theta + \dot{\sigma}_\theta^2) - \frac{C_0 p t^{p-1}}{3^{\eta_0 + 1}} (\sigma_\rho^2 - \sigma_\rho \sigma_\theta + \sigma_\theta^2) \times [\dot{\sigma}_\rho (2\sigma_\rho - \sigma_\theta) + \dot{\sigma}_\theta (2\sigma_\theta - \sigma_\rho)] \right\} r dr dz \qquad (14)$$

### Stress Resultants and Displacements

The manner in which the stresses are assumed to vary over the shell thickness is defined by Eqs. (4) in terms of the force and moment resultants. It is necessary, therefore, to determine the variation of these stress resultants and displacements along a meridian of the shell so that the spatial integrations indicated by Eq. (14) can be carried out.

Approximations to the stress resultants and displacements can be obtained by considering the forms of these quantities for the elastic case[2,3] and building into them a flexibility relative to time by means of dimensionless time parameters that then can be determined by the variational theorem.

The stress resultants and displacements are assumed to depend on time according to the relations

$$\begin{aligned} M_i(r,t) &= (DB/\rho_0^2) M'_i(r) M_i^*(t) \\ N_i(r,t) &= (Eh/R) B N'_i(r) N_i^*(t) \\ u(r,t) &= (\rho_0/R) B u'(r) u^*(t) \end{aligned} \qquad (15)$$

and

$$w(r,t) = B w'(r) w^*(t), \quad (i = \rho, \theta)$$

The primed quantities appearing in Eqs. (15) are dimensionless spatial stress resultants and displacements that depend only on the dimensionless radial coordinate $r$, and Poisson's ratio. Thus, aside from Poisson's ratio these quantities are independent of material and geometrical properties. The starred quantities represent dimensionless time parameters.

If the initial values of the dimensionless time parameters are taken as unity, $M_i^*(0) = 1$, $N_i^*(0) = 1$, $u^*(0) = 1$, $w^*(0) = 1$; then the time-varying stress resultants and displacements (15) reduce to those which occur immediately prior to creep, i.e., to the elastic values of these quantities.[2,3] Formulas for the stress resultants and displacements, as given by the elastic shallow shell theory, involve the zeroth- and first-order Kelvin functions and therefore are unsuitable

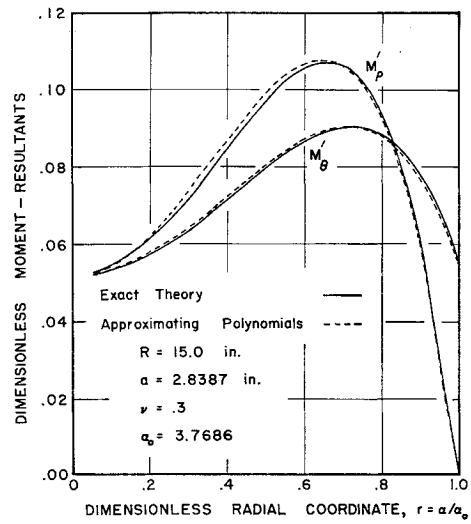


**Fig. 2 Comparison of approximating polynomials for space-varying dimensionless moment resultants, $M'_\rho$ and $M'_\theta$, with exact values from thin shallow spherical shell theory.**

for use in Eq. (14) because of the difficulties encountered in the integration of this equation. Consequently, the spatial variations of the dimensionless stress resultants and displacements are approximated by simple polynomials

$$M'_\rho(r) = (1 - r^2)(A_1 + A_2 r^2) \qquad (16a)$$

$$M'_\theta(r) = A_3 + r^2(A_4 + A_5 r^2) \qquad (16b)$$

$$N'_\rho(r) = A_6 + A_7 r^2 \qquad (16c)$$

$$N'_\theta(r) = A_8 + A_9 r^2 \qquad (16d)$$

$$w'(r) = (1 - r^2)(A_{10} - A_{11} r^2) \qquad (16e)$$

and

$$u'(r) = A_{12} r(1 - r) \qquad (16f)$$

Comparisons between the approximating polynomials (16) and the exact values of the corresponding quantities given by Eqs. (B-3) through (B-8) of Appendix B are shown in Figs. 2, 3, and 4.

Employing Eqs. (15, 16, and 4), the creep functional (14) becomes

$$I = (I_1 N_\theta^* + I_2 N_\rho^*)(\dot{u}^*)^2 + (I_3 N_\theta^* + I_4 N_\rho^* + I_5 M_\theta^* + I_6 M_\rho^*)(\dot{w}^*)^2 + (I_7 N_\theta^* + I_8 N_\rho^* + I_9 M_\theta^* + I_{10} M_\rho^*) \dot{w}^* \dot{u}^* + I_{11} \dot{N}_\rho^* \dot{u}^* + I_{12} N_\theta^* \dot{u}^* + (I_{13} + I_{14} \dot{w}^*) \dot{N}_\rho^* \dot{w}^* + I_{15} \dot{N}_\theta^* \dot{w}^* + I_{16} \dot{M}_\rho^* \dot{w}^* + I_{17} \dot{M}_\theta^* \dot{w}^* + I_{18} (\dot{N}_\rho^*)^2 + I_{19} (\dot{N}_\theta^*)^2 + I_{20} (\dot{M}_\rho^*)^2 + I_{21} (\dot{M}_\theta^*)^2 + I_{22} \dot{N}_\rho^* \dot{N}_\theta^* + I_{23} \dot{M}_\rho^* \dot{M}_\theta^* + I_{24} K \dot{N}_\rho^* N_\rho^* + I_{25} K \dot{N}_\rho^* N_\theta^* + I_{26} K \dot{N}_\theta^* N_\theta^* + I_{27} K \dot{N}_\theta^* N_\rho^* + I_{28} K \dot{M}_\rho^* M_\rho^* + I_{29} K \dot{M}_\rho^* M_\theta^* + I_{30} K \dot{M}_\theta^* M_\theta^* + I_{31} \dot{M}_\theta^* M_\rho^* \qquad (17)$$

where $K = C_0 p t^{p-1}/3$. In arriving at this expression, $\eta_0$ has been set equal to zero. This corresponds to $m = 1$ in the uniaxial creep law. It was found in the experimental phase of the investigation that the family of constant stress creep curves associated with the material from which the test shells were constructed could be accurately represented by several sets of values of $\lambda$, $m$, $p$. Furthermore, any set of this sequence of sets of values of $\lambda$, $m$, $p$ represented the family of constant stress creep curves as accurately as any other set of the sequence. Thus, it was possible to choose $m = 1$, provided corresponding values of $\lambda$ and $p$ also were

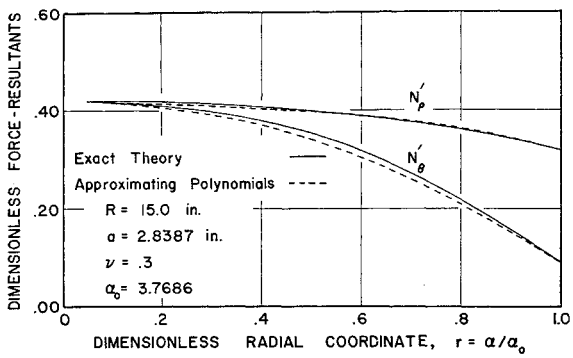


**Fig. 3 Comparison of approximating polynomials for space-varying dimensionless force resultants, $N'_\rho$ and $N'_\theta$, with exact values from thin shallow spherical shell theory.**

chosen. If $m$ cannot be set equal to unity with a resulting accurate representation of the family of constant stress creep curves, then integration of Eq. (14) becomes extremely difficult. Formulas for the constants $I_i$ appearing in Eq. (17) are given in Appendix C.

According to the variational theorem for creep the actual stress rates and velocities which occur for a known state of stress correspond to a stationary value of the creep functional. Consequently, setting the partial derivatives of the creep functional (14) with respect to the time rates of change of the various dimensionless time parameters equal to zero yields the following set of six linear first-order ordinary differential equations with time as the independent variable

$$2(I_1N_\theta^* + I_2N_\rho^*)\dot{u}^* + (I_7N_\theta^* + I_8N_\rho^* + I_9M_\theta^* + I_{10}M_\rho^*)\dot{w}^* + I_{11}\dot{N}_\rho^* + I_{12}\dot{N}_\theta^* = 0 \quad (18a)$$

$$(I_7N_\theta^* + I_8N_\rho^* + I_9M_\theta^* + I_{10}M_\rho^*)\dot{u}^* + (I_3N_\theta^* + I_4N_\rho^* + I_5M_\theta^* + I_6M_\rho^*)\dot{w}^* + (I_{13} + I_{14}w^*)\dot{N}_\rho^* + I_{15}\dot{N}_\theta^* + I_{16}\dot{M}_\rho^* + I_{17}\dot{M}_\theta^* = 0 \quad (18b)$$

$$I_{11}\dot{u}^* + (I_{13} + I_{14}w^*)\dot{w}^* + 2I_{18}\dot{N}_\rho^* + I_{22}\dot{N}_\theta^* = -K(I_{24}N_\rho^* + I_{25}N_\theta^*) \quad (18c)$$

$$I_{12}\dot{u}^* + I_{15}\dot{w}^* + I_{22}\dot{N}_\rho^* + 2I_{19}\dot{N}_\theta^* = -K(I_{27}N_\rho^* + I_{26}N_\theta^*) \quad (18d)$$

$$I_{16}\dot{w}^* + 2I_{20}\dot{M}_\rho^* + I_{23}\dot{M}_\theta^* = -K(I_{28}M_\rho^* + I_{29}M_\theta^*) \quad (18e)$$

$$I_{17}\dot{w}^* + I_{23}\dot{M}_\rho^* + 2I_{21}\dot{M}_\theta^* = -K(I_{30}M_\theta^* + I_{31}M_\rho^*) \quad (18f)$$

The set of equations (18) together with the initial conditions constitute an initial value problem which determines the dimensionless time parameters. A direct solution was not possible, consequently the solution was generated numerically using the fourth-order Runge-Kutta method.[5] The Runge-Kutta method requires that the derivatives at the initial point be finite; however, in the present case it is observed that $K \to \infty$ as $t$ approaches zero, and the Runge-Kutta method cannot be used to start the process. The method of Picard[5] permits, in this case, the calculation of the values of the dimensionless time parameters for a point in the immediate vicinity of $t = 0$. The Runge-Kutta method can then be employed to generate the remainder of the solution by using these new values as initial values.

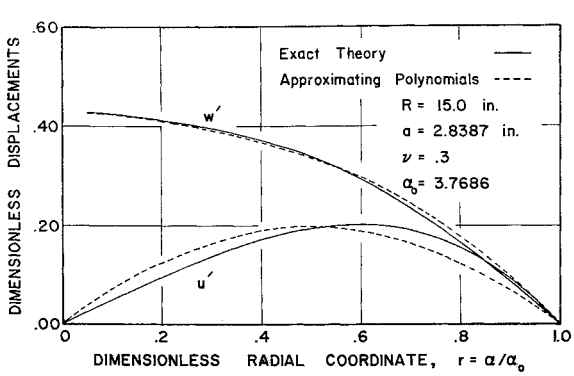


**Fig. 4 Comparison of approximating polynomials for space-varying dimensionless displacements, $u'$ and $w'$, with exact values from thin shallow spherical shell theory.**

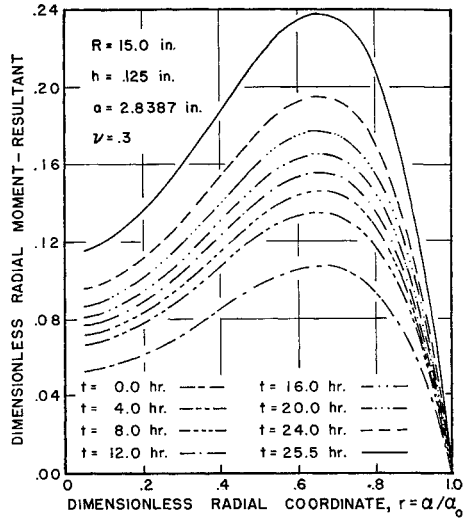


**Fig. 5 Time variation of the dimensionless radial moment resultant $M_\rho$ for an external pressure $q = 24$ psi.**

Figures 5 and 6 show the variation with time of the dimensionless radial moment and radial force resultants. It is observed that these stress resultants increase rapidly during the early stages of creep (transient creep), uniformly during the intermediate stages (steady-state creep), and rapidly again during the final stages prior to collapse. The graphs of the circumferential moment and force resultants exhibited the same behavior.

Figures 7, 8, and 9 show the dimensionless center deflection, $w/R$, as a function of time for external pressures of 20, 22, and 24 psi, respectively. Again, the transient, steady-state, and tertiary regions of creep are readily discernible. The configuration for which collapse occurs corresponds to the time for which the determinant of the coefficients for the standard form of the differential equations (18) vanishes.

## III. Experimental Results

The experimental phase of this investigation concentrated on obtaining: 1) accurate properties (both creep and elastic)

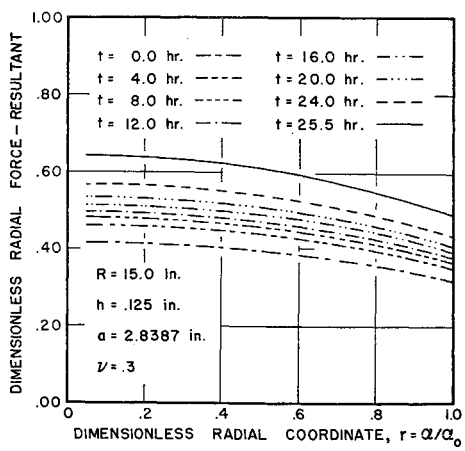


**Fig. 6 Time variation of the dimensionless radial force resultant $N_\rho$ for an external pressure $q = 24$ psi.**

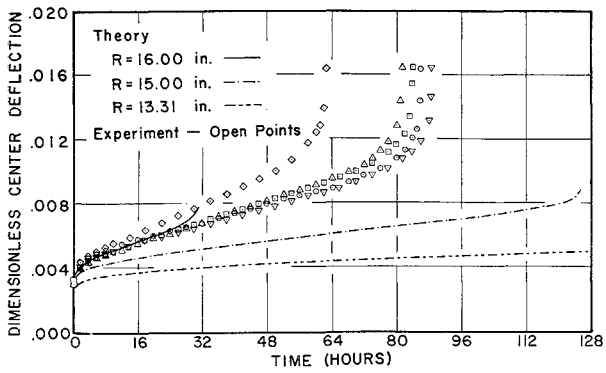


**Fig. 7 Comparison of the theoretical and experimental dimensionless center deflection $w/R$ for an external pressure $q = 20$ psi.**

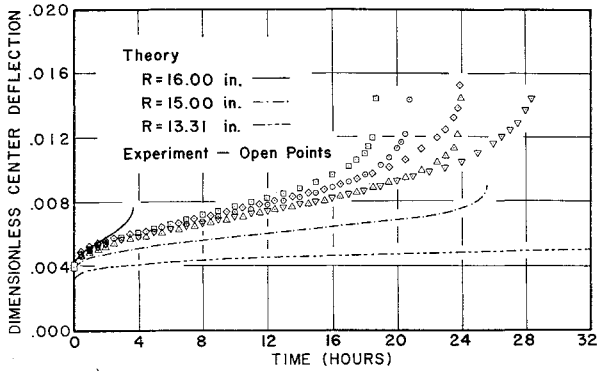


**Fig. 9 Comparison of the theoretical and experimental dimensionless center deflection $w/R$ for an external pressure $q = 24$ psi.**

for the material from which the test shells were made, and 2) accurate creep deflection and collapse time data for several test shells at three different pressure levels.

### Material Properties

The theory developed in the preceding section requires that the time-dependent properties $\lambda$, $m$, $p$ and the elastic properties $E$ and $\nu$ be known.

The creep properties were obtained by requiring the uniaxial creep relation

$$\epsilon = \lambda \sigma^m t^p \tag{19}$$

to closely approximate the family of constant stress tension creep curves for Type 6/6 Nylon shown in Fig. 10. Each shaded band in this figure represents the region into which the experimental data for six separate tests at the same stress level fell. The solid circles, triangles, etc., represent the predictions of Eq. (19) using the properties $p = 0.36$, $m = 1$, and $\lambda = 29.1 \times 10^{-8}$. It is observed that the experimental data is represented accurately by this relation.

The tension creep specimens were cut from the same sheet of material from which the test shells were constructed, and received the same heat treatment. Moreover, the tension creep tests were made in a laboratory for which the temperature and relative humidity were carefully controlled so as to coincide with the environment in which the data for the test shells were collected. Temperature and humidity were maintained at 70 ± 1°F and 40 ± 2%, respectively. Thus, the time-dependent properties used in the theoretical predictions should represent closely those associated with the test shells.

The modulus of elasticity and Poisson's ratio were found to be $E = 442{,}000$ psi and $\nu = 0.3$. Specimens used to obtain these data were taken from the group of tension creep specimens. However, it was not possible to make the required tests in the controlled atmosphere. Nevertheless, it is felt that the deviation in environments was small and had insignificant effects on the elastic properties.

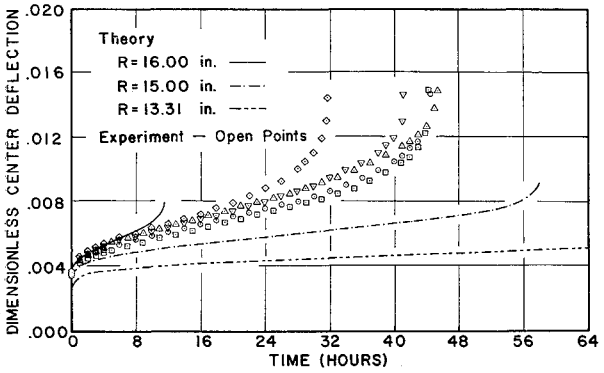


**Fig. 8 Comparison of the theoretical and experimental dimensionless center deflection $w/R$ for an external pressure of $q = 22$ psi.**

### Shell Creep Data

A pressure chamber was constructed so that experimental creep deflections and collapse times could be obtained for several test shells. The pressure chamber employed room temperature air as the loading medium and a Norgran Type 11-018 pressure regulator to maintain the desired pressure. The chamber consisted of a thick-wall steel tube with flanges welded to each end. Steel plates were bolted to these flanges; the upper plate being solid except where the air source and bleed-off connections were attached, whereas the lower plate contained a counterbored hole that served as the simple support for the test shell.

A $\frac{1}{4}$ in. aluminum plate with four radial slots located at 90° intervals was bolted to the lower plate. This provided a reference surface for an electrical deflectometer and four dial indicators measuring deflections at a constant distance from the pole of the shell and at 90° intervals around the shell. It also precluded an accidental discharge of the test shell from the pressure chamber. The center deflection was recorded continuously for five separate test shells at the same pressure level. Data were obtained for three different pressure levels of 20, 22, and 24 psi, and are presented in Figs. 7, 8, and 9.

The test shells were formed by heating flat disks of the required thickness (0.125 in.) in raw linseed oil for 7 hr at 365°F. It was necessary to use linseed oil in order to prevent oxygen embrittlement of the surface. The soft disks were clamped between specially made forming dies and allowed to cool slowly to room temperature. The edge of each shell was then machined to the proper dimension for insertion into the pressure chamber. Creep tests were begun for each test shell within 2 hr after machining the edge.

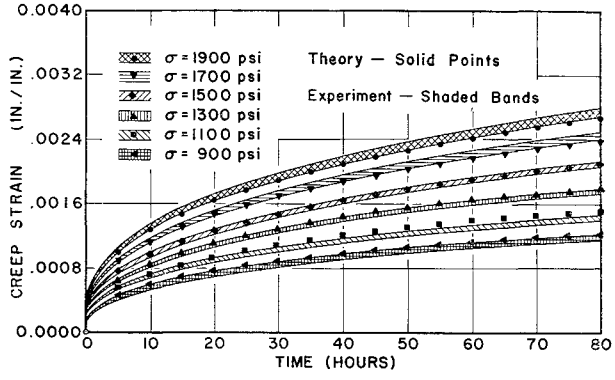


**Fig. 10 Experimental data for constant stress tension creep tests for Type 6/6 Nylon at 70°F.**

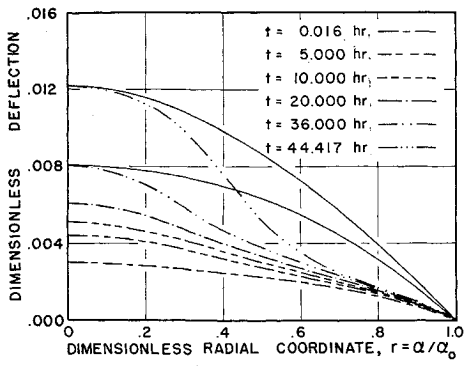


**Fig. 11 Comparison of experimental and theoretical mode forms for dimensionless transverse displacements $w/R$ at various times for a pressure of 22 psi.**

## IV. Discussion and Conclusions

Figure 7 displays the theoretical predictions for the creep deflections and collapse times for several values of the radius $R$ for a pressure of 20 psi. The unconnected points represent experimental data obtained for five test shells. Figures 8 and 9 display the same information for pressures of 22 and 24 psi, respectively. The experimental data correspond to test shells which were formed in dies of mean radius 11.875 in.; however, theoretical predictions for this radius are not shown since, without exception, the test shells became more convex (opened) upon removal from the forming dies. After the test shells were placed in the pressure chamber no-load measurements of the vertical distance from the reference base to the internal surface of the shell were made at $\alpha = 0$, 0.62, and 1.0. Using this measured data, it was found that the test shells were not perfectly spherical; however, the deviation from sphericity was small and the radii of the test shells were calculated to be very nearly 13.31 in. The observation that the radii were approximately the same for all test shells is substantiated to some extent by the relatively small amount of scatter in the creep data for most of the test shells.

Unfortunately, the theoretical predictions, based on the variational theorem for creep, for a radius of 13.31 in. do not agree closely with the experimental data. Consequently, theoretical predictions for radii of 15 and 16 in. also are presented for each pressure level so that the sensitivity of the theory to small changes in radius is displayed. It is apparent that the theoretical creep deflections and collapse times depend significantly on the radius of the shell; however, it is felt that the radius of 13.31 in. represents very closely the actual radius of the shell and hence one must search elsewhere for the source of the discrepancy between the theoretical predictions and the experimental data.

In order to ascertain where significant improvements in the comparison of the theoretical predictions and the experimental data might be made it is necessary to bring into focus certain assumptions used in the construction of the conceptual creep model as well as any deviations that the experimental models may have had from the conceptual model.

Aside from the usual kinematic assumptions of shallow shell theory there are three aspects of the conceptual model whose effects on the theoretical creep predictions should be discussed. The first centers on the validity of the constitutive relation used to represent the creep behavior of the material from which the test shells were constructed. The constitutive relation employed in this study has been accepted on the basis of its use in other creep studies of a similar nature. Unfortunately, the authors have been unable to uncover experimental evidence confirming or refuting its validity. The effect of the constitutive relation on the comparison between the theoretical predictions and the experimental data depends on how severely the constitutive relation fails to represent the correct creep behavior of the material from which the test shells were constructed.

The second aspect centers on the choice of the form of the time-dependence of the functions (15) used to represent the stress resultants and displacements after the onset of creep. The nature of these functions is such that they reduce approximately to the stress resultants and displacements at $t = 0$ in accordance with shallow spherical shell theory. Now as the test shell deforms with the passage of time the shapes of the graphs of the stress resultants and displacements change. Since only a single time parameter is built into each of the functions (15) one suspects that for short times these approximate stress and displacement mode forms represent accurately the actual stress and displacement mode forms. However, with the passage of time, the deviation between the approximate and the actual stress and displacement mode forms can become serious. Figure 11 indicates the extent of this deviation for the transverse deflection in the present study. The broken lines represent the experimental mode forms for various times, whereas the solid lines represent the theoretical mode forms. Since the theoretical mode forms have the same shape for all times it is observed that the two mode forms are essentially the same for short times but deviate increasingly for longer times. Moreover, it is noted that the theoretical and actual mode forms for the bending moments would be similar to those for the transverse deflection and would exhibit similar deviations. A significant improvement in the comparison between the theoretical creep predictions and the experimental data can be obtained by taking the stress resultants and displacements in the form of power series in the dimensionless radial coordinate with time-dependent coefficients. Naturally, the more terms that are retained in these series the greater will be the number of dependent variables in the system of differential equations governing the creep behavior of the shell. Thus, practical considerations will determine the number of terms that can be retained.

Finally, the conceptual model embodied the assumption that both the elastic and creep deformations occurred in a rotationally symmetric manner. The deflections of the test shells were measured at 90° intervals on a circle corresponding to $\alpha = 0.62$ for various times. The differences between the deflection at these four points were insignificant for small times, and increased to a maximum of 3.26% in the region just prior to collapse. Consequently, the assumption of rotationally symmetric deformations is considered valid.

In conclusion, it is felt that the discrepancy observed between the theoretical predictions for the creep deflections and collapse times and the experimental data is due principally to the deviations that occur between the theoretical and actual stress and displacement mode shapes with the passage of time. Closer agreement is to be expected when more time flexibility is built into these mode forms.

## Appendix A: Transformation of $\dot{U}_{k,i}\dot{U}_{k,j}\sigma_{ij}$

Unlike the other terms in the integrand of the volume integral, the term $\dot{U}_{k,i}\dot{U}_{k,j}\sigma_{ij}$ is not invariant under a transformation of coordinates and must be transformed to the system of coordinates $(\rho,\theta,z)$ used in this investigation. It is convenient to transform this term to spherical coordinates $r, \phi, \nu$ (radial distance, colatitude, and longitude, respectively) and later replace them with the shallow shell coordinates $(\rho,\theta,z)$.

Let the transformation of coordinates be designated by $x_i = x_i(x_\alpha)$, where Latin subscripts refer to the original (Cartesian) set of axes and Greek subscripts to the final set of axes, then

$$\dot{U}_{k,i}\dot{U}_{k,j}\sigma_{ij} = \left(\frac{\partial \dot{U}_k}{\partial x_\alpha}\frac{\partial x_\alpha}{\partial x_i}\right)\left(\frac{\partial \dot{U}_k}{\partial x_\beta}\frac{\partial x_\beta}{\partial x_j}\right)\sigma_{ij} \qquad \text{(A1)}$$

Now if $\ell_{i\alpha}$ denote the direction cosines defining the orientation of the final set of axes with the initial set and $A_\alpha$ are scalar factors there may be written

$$dx_\alpha = (\ell_{i\alpha}/A_\alpha)dx_i \tag{A2}$$

with the aid of which Eq. (A1) becomes

$$\dot{U}_{k,i}\dot{U}_{k,j}\sigma_{ij} = \frac{\partial \dot{U}_k}{\partial x_\alpha}\frac{\partial \dot{U}_k}{\partial x_\beta}\frac{1}{A_\alpha A_\beta}(\ell_{i\alpha}\ell_{j\beta}\sigma_{ij}) \tag{A3}$$

The quantity in parentheses is just $\sigma_{\alpha\beta}$; consequently, there is obtained

$$\dot{U}_{k,j}\dot{U}_{k,j}\sigma_{ij} = \frac{\partial \dot{U}_k}{\partial x_\alpha}\frac{\partial \dot{U}_k}{\partial x_\beta}\frac{1}{A_\alpha A_\beta}\sigma_{\alpha\beta} \tag{A4}$$

For spherical coordinates $A_r = 1$, $A_\phi = r$, and $A_\theta = r\sin\phi$. Thus, there results for the present study ($\sigma_r = \tau_{r\theta} = \tau_{r\phi} = \tau_{\phi\theta} = 0$)

$$\dot{U}_{k,i}\dot{U}_{k,i}\sigma_{ij} = \frac{\dot{U}_\phi^2 + \dot{V}_\phi^2 + \dot{W}_\phi^2}{r}\sigma_\rho + \frac{\dot{U}_\theta^2 + \dot{V}_\theta^2 + \dot{W}_\theta^2}{r^2\sin^2\phi}\sigma_\theta \tag{A5}$$

Making use of the transformation $U_i = l_{i\alpha}U_\alpha$ and assuming displacements that vary according to the relations $U = u - zw$, $W = w$, and $V = 0$, relation (A5) reduces to the required expression in shallow shell coordinates;

$$\dot{U}_{k,i}\dot{U}_{k,j}\sigma_{ij} = \left(\frac{\dot{w}}{R} + \frac{\dot{u}}{\rho} - \frac{z}{\rho}\dot{w}_\rho\right)^2\sigma_\theta + \left[\left(\frac{\dot{w}}{R} + \dot{u}_\rho - z\dot{w}_{\rho\rho}\right)^2 + \left(\dot{w}_\rho - \frac{\dot{u}}{R} + \frac{z}{R}\dot{w}_\rho\right)^2\right]\sigma_\rho \tag{A6}$$

The last expression has been obtained making use of the approximations $(\rho/R)^2 - 1$ and $z/R \ll 1$.

However, the special form of these formulas relevant to the present study are listed below. For convenience these formulas have been nondimensionalized. Thus, if the primed quantities refer to the nondimensional quantities, we shall have for the simply supported shallow spherical shell under uniform external pressure $q$ the following formulas:

$$M'_\rho = M_\rho\frac{\rho_o^2}{D}B = C_1\left[bei\alpha + \frac{1-\nu}{2^{1/2}\alpha}(ber_1\alpha + bei_1\alpha)\right] + C_2\left[ber\alpha - \frac{1-\nu}{2^{1/2}\alpha}(-ber_1\alpha + bei\alpha)\right] \tag{B3}$$

$$M'_\theta = M_\theta\frac{\rho_0^2}{D}B = C_1\left[\nu bei\alpha - \frac{1-\nu}{2^{1/2}\alpha}(ber_1\alpha + bei_1\alpha)\right] - C_2\left[\nu ber\alpha + \frac{1-\nu}{2^{1/2}\alpha}(-ber_1\alpha + bei_1\alpha)\right] \tag{B4}$$

$$N'_\rho = N_\rho\frac{R}{Eh}B = \frac{1}{2^{1/2}\alpha}[C_1(-ber_1\alpha + bei_1\alpha) - C_2(ber_1\alpha + bei_1\alpha)] + \frac{1}{(1-\nu)\alpha_0} \tag{B5}$$

$$N'_\theta = N_\theta\frac{R}{Eh}B = C_1\left[ber\alpha - \frac{1}{2^{1/2}\alpha}(-ber_1\alpha + bei_1\alpha)\right] + C_2\left[bei\alpha + \frac{1}{2^{1/2}\alpha}(ber_1\alpha + bei_1\alpha)\right] + \frac{1}{(1-\nu)\alpha_0} \tag{B6}$$

$$u' = u\frac{R}{\rho_0}B = \frac{1+\nu}{2}[-C_1(-ber_1\alpha + bei_1\alpha) - C_2(ber_1\alpha + bei_1\alpha)] \tag{B7}$$

$$w' = w(B) = C_1\,ber\alpha + C_2\,bei\alpha + C_3 \tag{B8}$$

In the foregoing formulas $B = (1-\nu)\,qR^2\alpha_0/(2Eh)$ and the constants $C_i$ are given by the formulas

$$C_1 = -\frac{ber\alpha_0 - (1-\nu/2^{1/2}\alpha_0)(-ber_1\alpha_0 + bei_1\alpha_0)}{2^{1/2}[bei\alpha_0(ber_1\alpha_0 + bei_1\alpha_0) - ber_1\alpha_0(-ber_1\alpha_0 + bei_1\alpha_0)] + \alpha_0^2(ber^2\alpha_0 + bei^2\alpha_0) + \left(\frac{1-\nu^2}{\alpha_0}\right)(ber_1^2\alpha_0 + bei_1^2\alpha_0)} \tag{B9}$$

$$C_2 = \frac{bei\alpha_0 + \frac{1-\nu}{2^{1/2}\alpha_0}(ber_1\alpha_0 + bei_1\alpha_0)}{ber\alpha_0 - \frac{1-\nu}{2^{1/2}\alpha_0}(-ber_1\alpha_0 + bei_1\alpha_0)}C_1 \tag{B10}$$

$$C_3 = -\{C_1\,ber\alpha_0 + C_2\,bei\alpha_0\} \tag{B11}$$

where $\alpha_0 = a/\rho_0$.

## Appendix B: Stress-Resultants and Displacements Associated with Elastic Shallow Shell Theory

Initial conditions associated with the simultaneous differential equations governing the creep behavior of thin shallow spherical shells are obtained from the elastic theory based on the equations of E. Reissner.[2] It is assumed that creep deformations do not begin until the total external pressure has been applied. Consequently, it is necessary to perceive the pressure to be applied instantaneously without introducing significant inertia effects. With this in mind, the initial conditions associated with the onset of creep are obtained from the elastic theory of shallow spherical shells. Only the results from this theory which are relevant to the present investigation are presented here.

The equations relevant to shallow spherical shells are

$$\nabla^4 w + (\rho_0^2/DR)\nabla^2\phi = q/(D\rho_0^4) \tag{B1}$$

$$\nabla^4\phi - (Eh/R)\rho_0^2\nabla^2 w = 0 \tag{B2}$$

Here $w$ and $\phi$ are the transverse displacement and Airy stress function, respectively, and are functions of the radial coordinate $\alpha = \rho/\rho_0$ in the base-plane of the shell. The parameter $\rho_0$ is defined by $\rho_0^4 = DR^2/(Eh)$, and $\rho$ is the radial coordinate in the base-plane of the shell.

Formulas for the stress resultants are given by E. Reissner[2,3] and will not be listed here because of space requirements.

## Appendix C: Coefficients Arising Through Integration of Creep Functional

$$I_1 = \frac{Eh\rho_0^2}{24R^3a^2}BA_{12}^2\left\{A_8 + \frac{1}{5}A_9\right\}$$

$$I_2 = \frac{Eh\rho_0}{12R^3}BA_{12}^2\left\{A_6\left(\frac{1}{a} + \frac{1}{10}\frac{\rho_0}{R^2}\right) + A_7\left(\frac{7}{10}\frac{1}{a} + \frac{1}{28}\frac{\rho_0}{R^2}\right)\right\}$$

$$I_3 = \frac{Eh}{12R}B\left\{A_{10}^2\left[A_8\left(\frac{1}{R^2} + 3\frac{h^2}{a^4}\right) + \frac{1}{2}A_9\left(\frac{1}{2R^2} + \frac{h^2}{a^4}\right)\right] + A_{10}A_{11}\left[A_8\left(\frac{1}{2R^2} - 4\frac{h^2}{a^4}\right) + A_9\left(\frac{1}{5R^2} + \frac{h^2}{3a^4}\right)\right] + A_{11}^2\left[A_8\left(\frac{1}{10R^2} + \frac{7}{3}\frac{h^2}{a^4}\right) + \frac{1}{2}A_9\left(\frac{1}{10R^2} + \frac{h^2}{3a^4}\right)\right]\right\}$$

$$I_4 = \frac{Eh}{6R} B\left\{\frac{1}{R^2}\left[\frac{1}{2} A_{10}^2\left(A_6 + \frac{1}{4} A_7\right) + A_{10}A_{11}\left(\frac{1}{4} A_6 + \frac{1}{10} A_7\right) + \frac{1}{20} A_{11}^2\left(A_6 + \frac{1}{2} A_7\right)\right] - \frac{h^2}{2a^4}\left[A_{10}^2\left(A_6 + \frac{1}{2} A_7\right) + A_{10}A_{11}(4A_6 + 3A_7) + A_{11}^2\left(7A_6 + \frac{11}{2} A_7\right)\right] + \left(\frac{12}{a^2} + \frac{h^2}{R^2a^2}\right)\left[A_{10}^2\left(\frac{1}{4} A_6 + \frac{1}{6} A_7\right) + \frac{1}{6} A_{10}A_{11}(A_6 + A_7) + A_{11}^2\left(\frac{1}{12} A_6 + \frac{1}{15} A_7\right)\right]\right\}$$

$$I_5 = \frac{D}{R\rho_0^2 a^2} B\left\{\frac{1}{2} A_{10}^2\left(A_3 + \frac{1}{3} A_4 + \frac{1}{6} A_5\right) + A_{10}A_{11}\left(\frac{1}{12} A_4 + \frac{1}{15}\right) A_5 + \frac{1}{60} A_{11}^2(A_4 + A_5)\right\}$$

$$I_6 = \frac{D}{60Ra^2\rho_0^2} B\{A_{10}^2(40A_1 + 15A_2) + A_{10}A_{11}(15A_1 + 13A_2) + A_{11}^2(11A_1 + 6A_2)\}$$

$$I_7 = \frac{Eh\rho_0}{R^3 a} BA_{12}\left\{A_{10}\left(\frac{7}{60} A_8 + \frac{11}{420} A_9\right) + A_{11}\left(\frac{11}{420} A_8 + \frac{5}{504} A_9\right)\right\}$$

$$I_8 = \frac{Eh\rho_0}{R^3 a} BA_{12}\left\{\frac{1}{12} A_{10}\left(A_6 + \frac{1}{6} A_7\right) - A_{11}\left(\frac{1}{28} A_6 + \frac{1}{72} A_7\right)\right\}$$

$$I_9 = \frac{D}{Ra^3\rho_0} BA_{12}\left\{A_{10}\left(\frac{1}{3} A_3 + \frac{1}{10} A_4 + \frac{1}{21} A_5\right) - A_{11}\left(\frac{2}{15} A_3 + \frac{1}{210} A_4 - \frac{1}{126} A_5\right)\right\}$$

$$I_{10} = \frac{D}{Ra\rho_0} BA_{12}\left\{A_{10}\left[A_1\left(-\frac{7}{210a^2} - \frac{11}{210}\frac{1}{R^2}\right) + A_2\left(-\frac{13}{210a^2} - \frac{5}{252R^2}\right)\right] + A_{11}\left[A_1\left(\frac{-71}{210a^2} + \frac{4}{315R^2}\right) + A_2\left(\frac{68}{210a^2} + \frac{1}{1540R^2}\right)\right]\right\}$$

$$I_{11} = -Eh\rho_0/R^2 a\, A_{12}\{\tfrac{1}{6} A_6 + \tfrac{3}{20} A_7\}$$

$$I_{12} = Eh\rho_0/R^2 a\, A_{12}\{\tfrac{1}{6} A_8 + \tfrac{1}{20} A_9\}$$

$$I_{13} = \frac{Eh}{4R^2}\left\{A_{10}\left(A_6 + \frac{1}{3} A_7\right) + A_{11}\left(\frac{1}{3} A_6 + \frac{1}{6} A_7\right)\right\}$$

$$I_{14} = \frac{Eh}{3Ra^2} B\left\{A_{10}^2(3A_6 + 2A_7) + 2A_{10}A_{11}(A_6 + A_7) + A_{11}^2\left(A_6 + \frac{4}{5} A_7\right)\right\}$$

$$I_{15} = \frac{Eh}{12R^2}\left\{A_{10}(3A_8 + A_9) + A_{11}\left(A_8 + \frac{1}{2} A_9\right)\right\}$$

$$I_{16} = -\frac{D}{a^2\rho_0^2}\left\{A_{10}\left(\frac{1}{2} A_1 + \frac{1}{6} A_2\right) + A_{11}\left(\frac{1}{2} A_1 + \frac{1}{3} A_2\right)\right\}$$

$$I_{17} = \frac{D}{a^2\rho_0^2}\left\{A_{10}\left(A_3 + \frac{1}{2} A_4 + \frac{1}{3} A_5\right) + \frac{1}{6} A_{11}(A_4 + A_5)\right\}$$

$$I_{18} = -Eh/12R^2\{3A_6^2 + 3A_6A_7 + A_7^2\}$$

$$I_{19} = -Eh/12R^2\{3A_8^2 + 3A_8A_9 + A_9^2\}$$

$$I_{20} = -\frac{D^2}{Eh^3\rho_0^4}\left\{A_1^2 + \frac{1}{2} A_1A_2 + \frac{1}{10} A_2^2\right\}$$

$$I_{21} = -\frac{D^2}{Eh^3\rho_0^4}\left\{3A_3(A_3 + A_4) + A_4\left(A_4 + \frac{3}{2} A_5\right) + A_5\left(\frac{3}{5} A_5 + 2A_3\right)\right\}$$

$$I_{22} = \frac{\nu Eh}{2R^2}\left\{A_6\left(A_8 + \frac{1}{2} A_9\right) + A_7\left(\frac{1}{2} A_8 + \frac{1}{3} A_9\right)\right\}$$

$$I_{23} = \frac{\nu D^2}{Eh^3\rho_0^4}\left\{A_1\left(3A_3 + A_4 + \frac{1}{2} A_5\right) + A_2\left(A_3 + \frac{1}{2} A_4 + \frac{3}{10} A_5\right)\right\}$$

$$I_{24} = 4EI_{18}, \quad I_{25} = \frac{E}{\nu} I_{22}, \quad I_{26} = 4EI_{19}, \quad I_{27} = \frac{E}{\nu} I_{22}$$

$$I_{28} = 4EI_{20}, \quad I_{29} = \frac{E}{\nu} I_{23}, \quad I_{30} = 4EI_{21}, \quad I_{31} = \frac{E}{\nu} I_{23}$$

## References


[1] Sanders, J. L., Jr., McCombe, H. G., Jr., and Schlechte, F. R., "A Variational Theorem for Creep with Applications to Plates and Columns," TN 4003, May 1957, NACA.

[2] Reissner, E., "Stresses and Displacements of Shallow Spherical Shells II," *Journal of Mathematics and Physics*, Vol. XXV, No. 1, Feb. 1946, pp. 279–300.

[3] Reissner, E., "Corrections to the Paper 'Stresses and Displacements of Shallow Spherical Shells II,'" *Journal of Mathematics and Physics*, Vol. XXVII, 1948, p. 240.

[4] Langhaar, H. L., "Energy Methods in Applied Mechanics," Wiley, New York, 1962, p. 183.

[5] Scarborough, J. B., "Numerical Mathematical Analysis," The Johns-Hopkins Press, Baltimore, 1958.